Thermal Diffusivity of Polyolefins by Temperature Wave Analysis

H. J. Chang, J. Morikawa, T. Hashimoto

Graduate School of Science and Engineering, Tokyo Institute of Technology, 2-12-1-S8, O-Okayama, Meguro-ku, Tokyo 152-8552, Japan

Received 10 August 2004; accepted 24 January 2005
DOI 10.1002/app.22102
Published online in Wiley InterScience (www.interscience.wiley.com).

ABSTRACT: The thermal diffusivities of 25 kinds of polyolefin films, including high-density polyethylene, low-density polyethylene, linear low-density polyethylene, polypropylene, 4-methylpentene, and ethylene–octene copolymer, were determined by temperature wave analysis in a continuous temperature scan. The thermal diffusivity decreased with increasing temperature, and the temperature dependence was steeper in the solid state than in the melt state. A supercooling phenomenon was observed in the crystallization process during cooling. The thermal diffusivity of polyethylene in the solid state was in a good correlation with the density at room temperature, and a higher temperature coefficient was observed in high-density polyethylene with a higher thermal diffusivity. The influence of the catalyst system on the thermal diffusivity was also observed in the ethylene–octene copolymer. The thermal diffusivity was sensitive to the precise change in the microstructure of the crystalline polyolefin, which was influenced not only by the chemical structure but also by the thermal history. © 2005 Wiley Periodicals, Inc. J Appl Polym Sci 99: 1104–1110, 2006

Key words: metallocene catalysts; polyolefins; thermal properties; thin films

INTRODUCTION

Heat-transport properties, such as thermal diffusivity and thermal conductivity, of polyolefins are important from practical and theoretical viewpoints because the processing involves various kinds of heat treatments and the microstructures of polyolefins are formed during those processes. In particular, in the numerical simulation of temperature variation during the various kinds of processing, it is necessary to employ the data of thermal properties of polymers concerned with the phase transitions that occur during the processing. However, the reported data for temperature-dependent thermal properties have been limited, particularly for various kinds of polyolefins in the temperature range including the phase transitions and the molten state by a continuous temperature scan.

A number of measurement methods have been used to determine the thermal diffusivity of polymers, including the photoacoustic method,[1–4] laser-flash method,[5–8] and modified hot wire method.[9,10] The temperature wave analysis (TWA) method[9–12] is advantageous for the measurement of the thermal diffusivity of thin films with a small area in the temperature range from the solid state to the molten state, including the melting and crystallization processes.

In this study, the TWA method was applied to the measurement of the temperature dependence of the thermal diffusivity of 25 kinds of polyolefins, including high-density polyethylene (HDPE), low-density polyethylene (LDPE), linear low-density polyethylene (LLDPE), polypropylene (PP), 4-methylpentene (4MP), and ethylene–octene copolymers. The influence of the metallocene and Ziegler–Natta catalyst systems on the thermal diffusivity was also examined for ethylene–octene copolymers.

EXPERIMENTAL

Samples

HDPE [density (ρ) = 954–970 kg/m^3, melt index (MI) = 0.4–13 g/10 min], LLDPE (ρ = 915–930 kg/m^3, MI = 2.3–18 g/10 min), LDPE (ρ = 916–920 kg/m^3, MI = 1.9–23 g/10 min), PP (ρ = 910 kg/m^3, MI = 1.8–11 g/10 min), and 4MP are listed in Table I with the commercial grade and the manufacturers. Ethylene–octene copolymers are listed in Table II with the comonomer content and the catalyst systems. The comonomer content was 2–24 wt %; the catalyst systems were metallocene and Ziegler–Natta systems.

Measurements

A schematic diagram of the experimental arrangement of the TWA method is shown in Figure 1. By the passage of a sine wave current supplied by an NF

Correspondence to: T. Hashimoto (toshimas@o.cc.titech.ac.jp).

TABLE I
Characteristics of the Polyolefins

Sample	Grade	Manufacturer	ρ (kg/m^3)	MI (g/10 min)
HDPE	7000F (1)	Mitsui Chemical Co., Ltd. (Tokyo, Japan)	956	0.04
	6200B (2)		958	0.36
	5000S (3)		954	0.8
	2200J (4)		968	5.2
	1300J (5)		965	13
	Sholex7150 (6)	Showadenko K. K. (Tokyo, Japan)	970	-
LLDPE	1520L (7)		915	2.3
	2520F (8)		925	2.3
	3520L (9)		930	2.3
	20200J (10)		920	18
LDPE	50 (11)	Mitsui Chemical Co., Ltd. (Tokyo, Japan)	920	1.9
	11P (12)		917	7.2
	68 (13)		916	23
PP	J340 (14)[a]		910	1.8
	F601 (15)[b]		910	6.5
	J700 (16)[b]		910	11
4-MP	RT18 (17)		-	-
	MX002 (18)		-	-

[a] PP block copolymer.
[b] PP homopolymer.

Electronic Industry (Yokohama, Japan) 1920 function synthesizer, a temperature wave, generated at the front surface of the specimen, was propagated in the thickness direction to the rear surface of the specimen. The temperature variation on the rear surface was detected with the variation of the electrical resistance of the sensor by an NF Electronic Industry 5610B lock-in amplifier as a phase delay and an amplitude decay. The specimen was inserted into the flat plates of the borosilicate glass, on which thin metal layers were directly sputtered, one as a heater and the other as a sensor. The specimen was once melted in the cells for better contact with the sensor and the heater, with a spacer to keep a constant thickness. The specimen thickness was 25–100 μm.

The thermal diffusivity (α) was calculated from the relationship of the square root of the angular frequency ($\sqrt{\omega}$) and the phase delay ($\Delta\theta$) of the temperature wave, as shown in eq. (1).

$$\Delta\theta = -\sqrt{\frac{\omega}{2\alpha}} \times d - \frac{\pi}{4} \tag{1}$$

where d is the thickness of the sample.

From eq. (1), the phase delay of the temperature wave shows a linear relationship with the square root of the angular frequency. The thermal diffusivity is calculated from the slope of the phase delay versus the square root of the angular frequency. The details of the principle of the TWA method are described in refs. 11–14.

This work also deals with the continuous measurement of the thermal diffusivity in a temperature scan by the TWA method. As shown in eq. (2), the thermal diffusivity can be calculated directly from the phase delay of each angular frequency as a function of the temperature:

$$\alpha = \frac{d^2\omega}{2\left(\Delta\theta + \frac{\pi}{4}\right)^2}. \tag{2}$$

The continuous temperature scan was also carried out during the melt-crystallization process at a rate of

TABLE II
Characteristics of the Ethylene-Octene (EO) Copolymers

Sample	Grade	Manufacturer	ρ (kg/m^3)	MI (g/10 min)	Octene (wt %)
EO copolymer (metallocene)	HF1030 (19)	Dow Chemical Japan Co., Ltd. (Tokyo, Japan)	936	2.5	2
	FM1570 (20)		916	1.0	7.5
	PL1880 (21)		902	1.0	12
	PF1140 (22)		896	1.6	14
	EG8100 (23)		870	1.0	24
EO copolymer (Ziegler–Natta)	2045 (24)		920	1.0	5–10
	4203 (25)		906	0.8	10–15

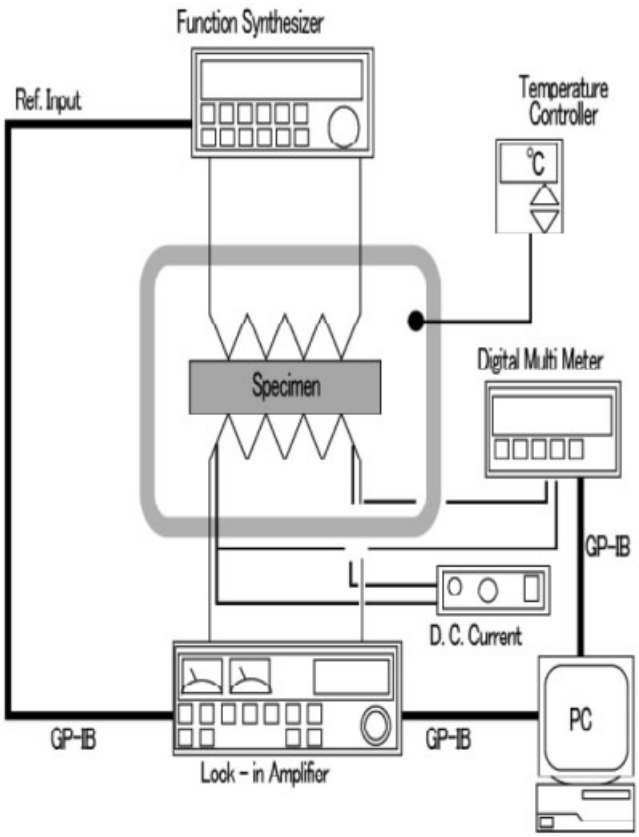

Figure 1 Schematic diagram of the experimental arrangement of the TWA method.

1°C/min. Before the measurement, the specimens were completely melted and cooled at a constant rate of 1°C/min. All measurements were performed as follows: the input voltage was less than 0.25 W/mm^2, and the measured frequency of TWA should have satisfied the thermally thick condition, $kd \gg 1$, where k is equal to $(\omega/2\alpha)^{1/2}$. The temperature calibration of TWA was performed with indium (film shape = 35 μm), which was calibrated with the onset temperature of differential scanning calorimetry (DSC) at a rate of 1°C/min.

The specimen holder was settled under a polarized optical microscope (Nikon, Tokyo, Japan), and the measurement of the thermal diffusivity was undertaken with an observation of the morphology during the phase transition of the polyolefin. The images were captured with a Nikon digital camera at various temperatures during the cooling and heating processes. These measurements were carried out at a constant rate of 1°C/min in a Mettler hot stage with a proportional integral difference (PID) temperature control.

DSC measurements were also carried out with a TAS200-DSC 8230D (Rigaku Electric Co., Ltd., Tokyo, Japan) under a dry nitrogen purge of 200 cc/min. The temperature scanning rate was 1°C/min, and the calibration was undertaken with indium, lead, and tin. Crystallinity (X_c) was calculated with a heat of fusion of 290 [polyethylene (PE)], 209 (PP), or 121.4 J/g (4MP) for the perfectly crystalline polymer.[15,16]

RESULTS AND DISCUSSION

Figure 2 shows the temperature dependence of the thermal diffusivity of HDPE, LDPE, and LLDPE, having nearly the same MI, in the cooling scan and the following heating scan. In the cooling process of HDPE, the thermal diffusivity increases with decreasing temperature in the molten state, and a steep change occurs during the crystallization. After a small peak, the thermal diffusivity increases more sharply in the solid state. The temperature dependence of the thermal diffusivity in heating can be observed in the same manner. The supercooling of the thermal diffusivity can be clearly observed. In the solid state, the thermal diffusivity of HDPE shows the highest value, which is related to the higher crystallinity (X_c = 0.72) compared with that of LDPE and LLDPE. A supercooling phenomenon can also be observed in LDPE during the crystallization process, but it cannot be clearly observed in LLDPE. In the order of crystallinity, the absolute value of the thermal diffusivity of LLDPE (X_c = 0.38) is higher than that of LDPE (X_c = 0.35) in the solid state. For HDPE, the value of the thermal diffusivity is almost the same as that obtained by Kamal et al.[9] in the solid state, whereas the thermal

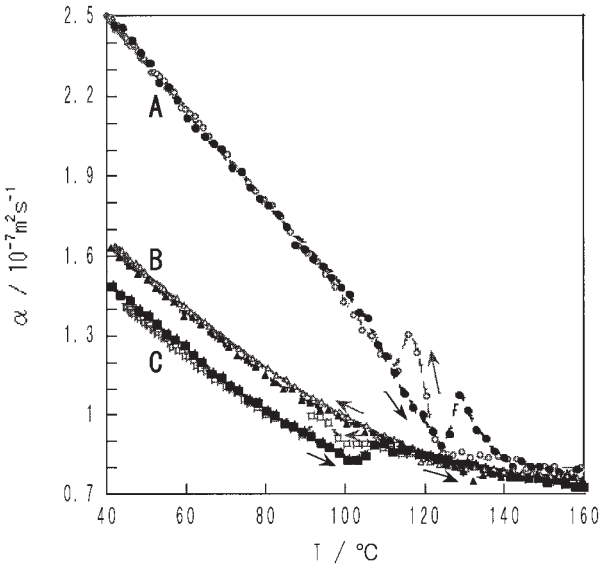

Figure 2 Temperature (T) dependence of the thermal diffusivity (α) of HDPE, LDPE, and LLDPE in the (○,△,□) cooling and (●,▲,■) heating processes at a scanning rate of 1°C/min: (A) no. 5 (HDPE, d = 23 μm, f = 246 Hz, MI = 13 g/10 min, ρ = 965 kg/m^3), (B) no. 10 (LLDPE, d = 26 μm, f = 184 Hz, MI = 18 g/10 min, ρ = 920 kg/m^3), and (C) no. 12 (LDPE, d = 26 μm, f = 138 Hz, MI = 7.2 g/10 min, ρ = 917 kg/m^3).

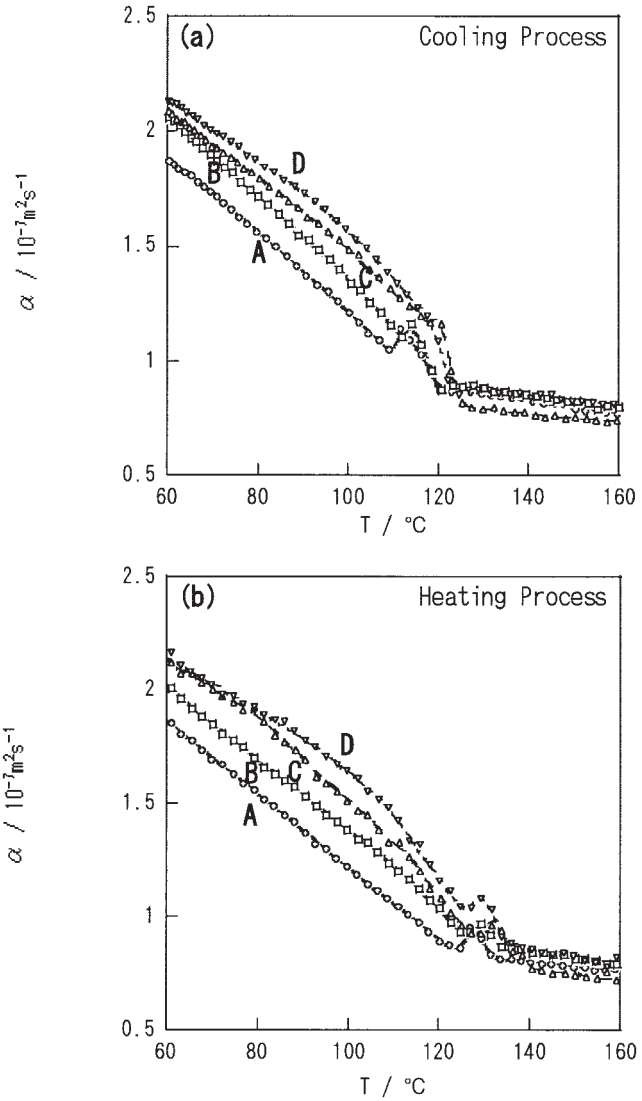

Figure 3 Temperature (T) dependence of the thermal diffusivity (α) of HDPEs of various densities in the (a) cooling and (b) heating processes at a scanning rate of 1°C/min: (A) no. 1 (d = 45 μm, f = 84 Hz, MI = 0.04 g/10 min, ρ = 956 kg/m^3), (B) no. 3 (d = 25 μm, f = 192 Hz, MI = 0.8 g/10 min, ρ = 954 kg/m^3), (C) no. 4 (d = 25 μm, f = 168 Hz, MI = 5.2 g/10 min, ρ = 968 kg/m^3), and (D) no. 6 (d = 26 μm, f = 264 Hz, ρ = 970 kg/m^3).

diffusivities of LLDPE and LDPE are about 25 and 30% lower, respectively, than those obtained by Zhang and Fujii[10] in the solid state. However, it is difficult to identify the differences between the measured data and the literature data because of insufficient data for the grade and the molecular structure between the polymers used in this article and the polymers used in the literature.

Figure 3 shows the temperature dependence of the thermal diffusivity of various densities of HDPE in the cooling scan and the subsequent heating scan. The measuring frequency was selected with consideration of the thermal diffusion length in each specimen. In the solid state, a higher value of the thermal diffusivity is obtained with a higher density of HDPE. Although the temperature dependence of the thermal diffusivity in the solid state depends on the density, the thermal diffusivities in the molten state are almost unchanged. A small peak in the phase transition and a supercooling can be observed in each specimen of HDPE.

Figure 4 shows the temperature dependence of the thermal diffusivity of ethylene–octene copolymers produced by the different metallocene and Ziegler–Natta systems, which have equal averaged octene contents. In the heating, the thermal diffusivity of the metallocene-catalyzed copolymer decreases with increasing temperature, and a small peak can be observed at 106–118°C, corresponding to the melting temperature (T_m) measured by DSC. In the molten state, the temperature dependence of the thermal diffusivity becomes smaller. However, the Ziegler–Natta copolymer shows a broader temperature dependence than that of the metallocene copolymer, and the melting process cannot be clearly observed. The absolute value of the thermal diffusivity of the Ziegler–Natta copolymer is higher than that of the metallocene copolymer. These different temperature dependences of the thermal diffusivity can be understood if we take into account the wide distribution of molecular weights and comonomer contents in the Ziegler–Natta catalyst.[17–22]

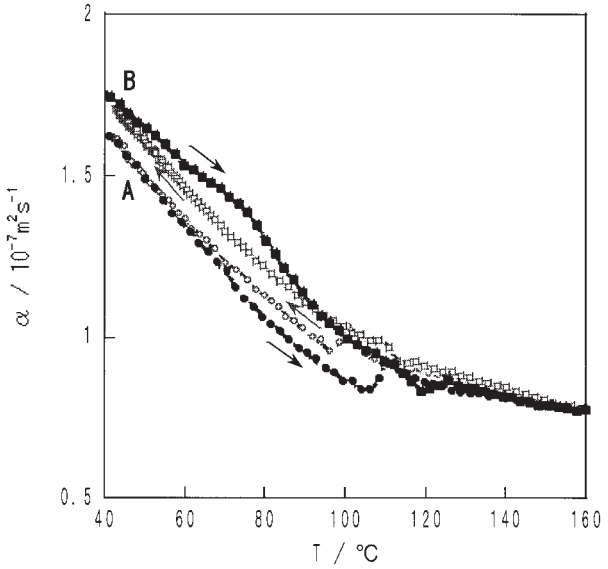

Figure 4 Temperature (T) dependence of the thermal diffusivity (α) of the ethylene–octene copolymer produced by the (A) metallocene and (B) Ziegler–Natta catalyst systems in the (○,□) cooling and (●,■) heating process at a scanning rate of 1°C/min: (A) no. 20 (metallocene, d = 54 μm, f = 54 Hz, MI = 1 g/10 min, ρ = 916 kg/m^3, octene content = 7.5 wt %) and (B) no. 24 (Ziegler–Natta, d = 27 μm, f = 124 Hz, MI = 1 g/10 min, ρ = 920 kg/m^3, octene content = 5–10 wt %).

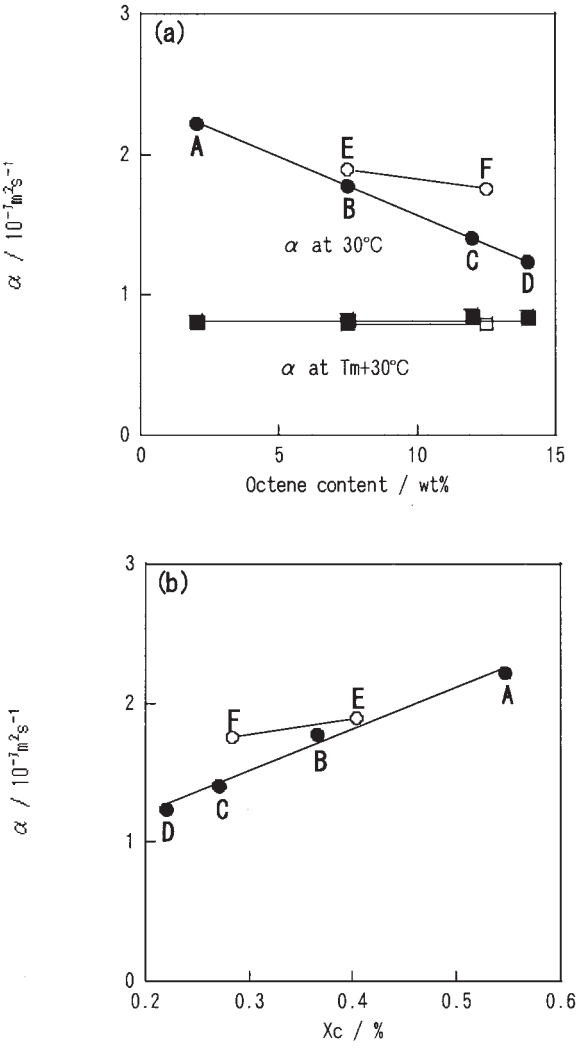

Figure 5 Variation of the thermal diffusivity (α) of the ethylene–octene copolymer at (●) 30°C and (■) at T_m + 30°C as a function of (a) the octene content and (b) X_c: (A) no. 19 (metallocene, octene content = 2 wt %, MI = 2.5 g/10 min, ρ = 936 kg/m^3), (B) no. 20 (metallocene, octene content = 7.5 wt %, MI = 1 g/10 min, ρ = 916 kg/m^3), (C) no. 21 (metallocene, octene content = 12 wt %, MI = 1 g/10 min, ρ = 902 kg/m^3), (D) no. 22 (metallocene, octene content = 14 wt %, MI = 1.6 g/10 min, ρ = 896 kg/m^3), (E) no. 24 (Ziegler–Natta, octene content = 5–10 wt %, MI = 1 g/10 min, ρ = 920 kg/m^3), and (F) no. 25 (Ziegler–Natta, octene content = 10–15 wt %, MI = 0.8 g/10 min, ρ = 906 kg/m^3).

Figure 5(a,b) shows the variation of the thermal diffusivity in the solid (30°C) and molten states (T_m + 30°C) as a function of the octene content and X_c, respectively. In the solid state, the thermal diffusivity of the metallocene copolymer decreases with increasing octene content. However, this tendency is not clear in Ziegler–Natta systems with equal averaged octene contents. In the molten state, the thermal diffusivity is an almost constant value, regardless of the octene content and the catalyst system.

Figure 6 shows a comparison of the temperature dependences of the thermal diffusivity of HDPE, PP, and 4MP, with not quite the same MI, in the cooling scan and subsequent heating scan. The thermal diffusivity shows the characteristic temperature dependence with the different molecular structures of the polymers. The thermal diffusivity in the solid state decreases with increasing temperature, and then the thermal diffusivity in the molten state decreases more gradually. Supercooling can be observed for each crystalline polymer. For the PP block copolymer [Fig. 6(B)], the increase in the thermal diffusivity during the crystallization is different from that obtained for the PP homopolymer [Fig. 6(C)]; a clear step increase of the thermal diffusivity cannot be found for the PP block copolymer. The values of the thermal diffusivity in the solid state are almost the same for the PP block copolymer and homopolymer. A similar tendency was observed by Zhang and Fujii.[10] The value of the thermal diffusivity at 30°C is 2.48 $\times$ 10^{-7} m^2/s for HDPE, 1.21 $\times$ 10^{-7} m^2/s for PP, and 1.26 $\times$ 10^{-7} m^2/s for 4MP.

The crystallization process of polyolefins was also investigated by the simultaneous measurement of the thermal diffusivity and the morphology observed under a polarized optical microscope. Figure 7 shows optical microscopy images of HDPE and PP at temperatures inserted in Figure 7(c) during the crystallization process. The change in the morphology observed under the sensor [the shadowed area in Fig.

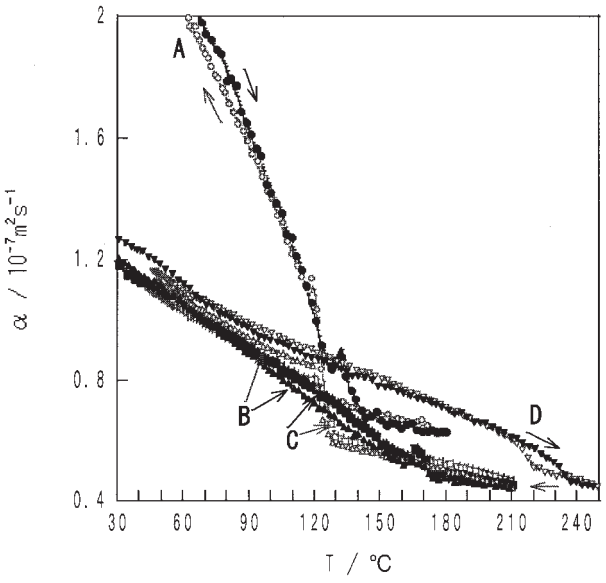

Figure 6 Temperature (T) dependence of the thermal diffusivity (α) of a set of HDPE, block copolymer PP, PP, and 4MP in the (○,△,□,▽) cooling and (●,▲,■,▼) heating processes at a scanning rate of 1°C/min: (A) no. 4 (HDPE, d = 25 μm, f = 168 Hz, MI = 5.2 g/10 min, ρ = 968 kg/m^3), (B) no. 14 (block copolymer PP, d = 22 μm, f = 106 Hz, MI = 1.8 g/10 min, ρ = 910 kg/m^3), (C) no. 15 (PP, d = 25 μm, f = 84 Hz, MI = 6.5 g/10 min, ρ = 910 kg/m^3), and (D) no. 17 (4MP, d = 26 μm, f = 118 Hz).

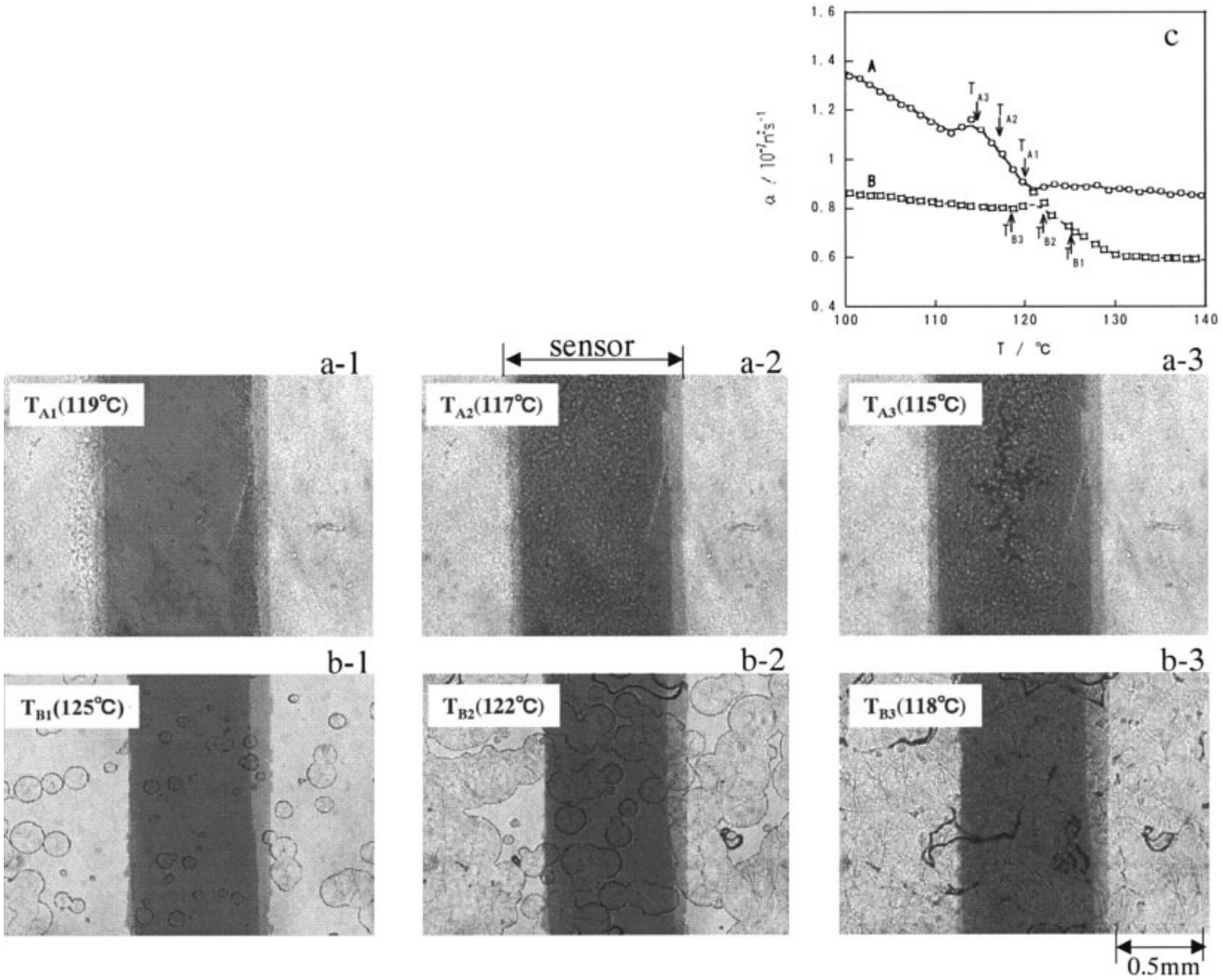

Figure 7 Optical microscopy images of HDPE and PP at various temperatures during the crystallization process: (A) no. 3 (HDPE, d = 25 μm, f = 84 Hz, MI = 0.8 g/10 min, ρ = 954 kg/m^3) and (B) no. 15 (PP, d = 25 μm, f = 84 Hz, MI = 6.5 g/10 min, ρ = 910 kg/m^3).

7(a,b)] corresponds to the change in the thermal diffusivity shown in Figure 7(c). When crystals appear from the molten state under the sensor, the thermal diffusivity starts to increase, and when the sensor area is filled with crystals, the slope of the temperature dependence of the thermal diffusivity changes. The crystal sizes are different for PE and PP (in this case, a small crystal for HDPE and a spherulite for PP). A coexistence state of the molten and solid states of these polymers in the crystallization process was observed as a change in the thermal diffusivity. The thermal diffusivity is sensitive to the changes in the microstructure formed during the crystallization process, especially the crystallinity and crystal size distribution.

Figure 8(a,b) shows the variation of the thermal diffusivity in the solid (30°C) and molten states (T_m + 30°C) plotted against the apparent density at room temperature and MI, respectively, for a series of HDPE, LDPE, LLDPE, ethylene–octene copolymer, and PP. In the solid state, the thermal diffusivity increases linearly with the apparent density. On the other hand, in the molten state, the thermal diffusivity of PE is almost constant, regardless of MI, but PP shows a much smaller value than a PE series. Figure 8(c) shows the temperature coefficient of the thermal diffusivity ($d\alpha/dT$) plotted against the thermal diffusivity at 30°C. With higher thermal diffusivity, a higher $d\alpha/dT$ value is obtained for the crystalline polyolefin. The phonon scattering in the crystalline part is thought to be more sensitive to temperature changes in the solid state of the polyolefin.

CONCLUSIONS

The TWA method was applied to the measurement of the thermal diffusivity of various kinds of poly-

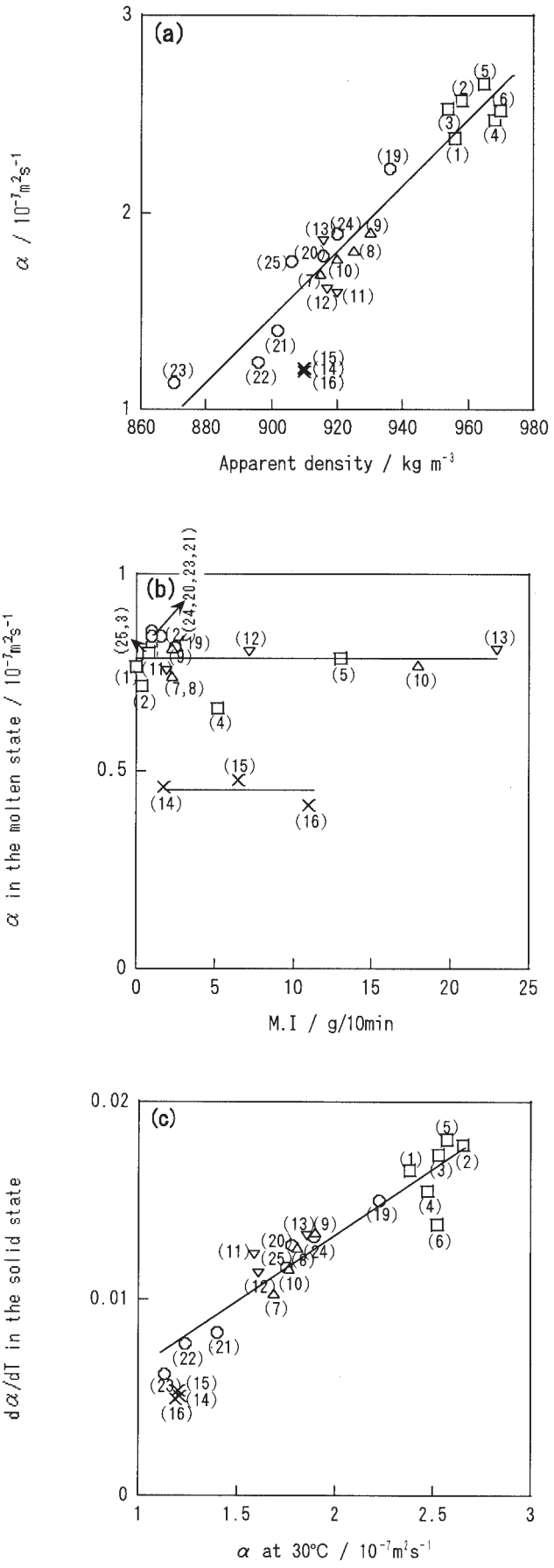

Figure 8 Variation of the thermal diffusivity (α) and temperature coefficient ($d\alpha/dT$) of polyolefins as a function of (a) ρ, (b) MI, and (c) α at 30°C.

olefins during a continuous temperature scan. The thermal diffusivity was sensitively obtained as a temperature-dependent thermal property, corresponding to the microstructure (crystallinity and crystal size distribution) in the solid state with a supercooling phenomenon in the phase-transition region. The thermal diffusivity of PE and ethylene–octene copolymer in the solid state was in a good correlation with the density but was mostly constant in the molten state. TWA is effective in detecting the precise changes of the thermal diffusivity of polyolefins, which is also influenced by the thermal history and the microstructure in the solid state.

References

1. Adams, M. J.; Kirkbright, G. F. Analyst 1977, 102, 678.
2. Leite, N. F.; Cella, N.; Vargas, H.; Miranda, L. C. M. J Appl Phys 1987, 61, 3025.
3. Torres-Filho, A.; Perondi, L. F.; Miranda, L. C. M. J Appl Polym Sci 1988, 35, 103.
4. Torres-Filho, A.; Leite, N. F.; Miranda, L. C. M.; Cella, N.; Vargas, H. J Appl Phys 1989, 66, 97.
5. Chen, F. C.; Poon, Y. M.; Choy, C. L. Polymer 1977, 18, 129.
6. Choy, C. L.; Luk, W. H.; Chen, F. C. Polymer 1978, 19, 155.
7. Choy, C. L.; Chen, F. C.; Luk, W. H. J Polym Sci Polym Phys Ed 1980, 18, 1187.
8. Choy, C. L.; Leung, W. P.; Ng, Y. K. J Polym Sci Part B: Polym Phys 1987, 25, 1779.
9. Kamal, M. R.; Tan, V.; Kashani, F. Adv Polym Technol 1982, 3, 89.
10. Zhang, X.; Fujii, M. Polym Eng Sci 2003, 43, 1755.
11. Morikawa, J.; Tan, J.; Hashimoto, T. Polymer 1995, 36, 4439.
12. Hashimoto, T.; Morikawa, J.; Kurihara, T.; Tsuji, T. Thermochim Acta 1997, 304, 151.
13. Kurihara, T.; Morikawa, J.; Hashimoto, T. Int J Thermophys 1997, 18, 505.
14. Jung, W. D.; Morikawa, J.; Hashimoto, T. Int J Thermophys 2000, 21, 503.
15. Yamakuchi, M.; Miyata, H.; Nitta, K. H. J Appl Polym Sci 1996, 62, 87.
16. Stark, P.; Lofgren, B. Eur Polym J 2002, 38, 97.
17. Kim, M. K.; Phillips, P. J. J Appl Polym Sci 1998, 70, 1893.
18. Simanke, A. G.; Galland, G. B.; Freitas, L.; Jornada, J. A. H. D.; Quijada, R.; Mauler, R. S. Polymer 1999, 40, 5489.
19. Androsch, R. Polymer 1999, 40, 2805.
20. Eynde, S. V.; Mathot, V. B. F.; Koch, M. H. J.; Reynaers, H. Polymer 2000, 41, 4889.
21. Jokela, K.; Vaanaen, A.; Torkkeli, T.; Starch, P.; Seimaa, R.; Lofgren, B.; Seppala, J. J Polym Sci Part B: Polym Phys 2001, 39, 1860.
22. Bensanson, S.; Nazarenko, S.; Chum, S.; Hillter, A.; Baer, E. Polymer 1997, 38, 3913.